



1 **Temperature variability of the Iberian Range since 1602**
2 **inferred from tree-ring records**

3

4

5 **E. Tejedor^{1,2,3}, M.A. Saz^{1,2}, J.M. Cuadrat^{1,2}, J. Esper³, M. de Luis^{1,2}**

6 [1]{University of Zaragoza, 50009 Zaragoza, Spain }

7 [2]{Environmental Sciences Institute of the University of Zaragoza }

8 [3]{Department of Geography, Johannes Gutenberg University, 55099 Mainz, Germany }

9 Correspondence to: E. Tejedor (etejedor@unizar.com)

10

11 **Abstract**

12 Tree-rings are an important proxy to understand the natural drivers of climate variability in
13 the Mediterranean basin and hence to improve future climate scenarios in a vulnerable region.
14 Here, we compile 316 tree-ring width series from 11 conifer sites in the western Iberian
15 Range. We apply a new standardization method based on the trunk basal area instead of the
16 tree cambial age to develop a regional chronology which preserves high to low frequency
17 variability. A new reconstruction for the 1602-2012 period correlates at -0.78 with
18 observational September temperatures with a cumulative mean of the 21 previous months
19 over the 1945-2012 calibration period. The new IR2T_{max} reconstruction is spatially
20 representative for the Iberian Peninsula and captures the full range of past Iberian Range
21 temperature variability. Reconstructed long-term temperature variations match reasonably
22 well with solar irradiance changes since warm and cold phases correspond with high and low
23 solar activity, respectively. In addition, some annual temperatures downturns coincide with
24 volcanic eruptions with a three year lag.

25

26 **1 Introduction**

27 The IPCC report (IPCC, 2013) highlighted a likely increase of average global temperatures in
28 upcoming decades, and pointed particularly to the Mediterranean basin, and therefore in the



1 Iberian Peninsula (IP), as a region of substantial modelled temperature changes. The
2 Mediterranean area is located in the transitional zone between tropical and extra-tropical
3 climate systems, characterized by a complex topography and high climatic variability (Hertig
4 and Jacobeit 2008). Taking into account these features, even relatively minor modifications of
5 the general circulation, i.e. a shift in the location of sub-tropical high pressure cells, can lead
6 to substantial changes in Mediterranean climate (Giorgi and Lionello 2008), making the study
7 area a potentially vulnerable region to anthropogenic climatic changes by anthropogenic
8 forces, i.e. increasing concentrations of greenhouse gases (Lionello et al., 2006a; Ulbrich et
9 al., 2006)

10 Major recent efforts have been made in understanding trends in temperatures throughout the
11 IP over the instrumental period (Kenaway et al., 2012; Pena-Angulo et al., 2015; Gonzalez-
12 Hidalgo et al., 2015) and future climate change scenarios (Sánchez et al., 2004; López-
13 Moreno et al., 2014). However, the fact that most of the observational records do not begin
14 until the 1950s (Gonzalez-Hidalgo et al., 2011) is limiting the possibility of investigating the
15 inter-annual to multi-centennial long-term temperature variability. Therefore, it is crucial to
16 explore climate proxy data and develop long-term reconstructions of regional temperature
17 variability to evaluate spatial patterns of climatic change and the role of natural and
18 anthropogenic forcings on climate variations (Büntgen et al., 2005). In the IP, much progress
19 has been made to reconstruct past centuries climate variability, including analysis of
20 documentary evidences for temperature (i.e. Camuffo et al., 2010) and droughts
21 reconstruction (i.e. Barriendos et al. 1997; Cuadrat and Vicente, 2007; Domínguez-Castro et
22 al., 2010). Additionally, progress has been made to further understanding of long-term climate
23 variability of the IP through dendroclimatological studies focussing on drought (Esper et al.,
24 2014; Tejedor et al., 2015) and temperature (Büntgen et al., 2008; Dorado-Liñán et al., 2012,
25 2014; Esper et al. 2015a). Nevertheless, a high-resolution temperature reconstruction for
26 central Spain is still missing.

27 Several studies have been made to develop a temperature reconstruction for the Iberian Range
28 (IR) using *Pinus uncinata* tree-ring data (Creus and Puigdefabreas, 1982; Ruiz, 1989). The
29 results, in fact, showed a pronounced inter-annual to century scale chronology variability.
30 However, their main result was a complex growth response function due to a mixed climate
31 signal instead of a temperature reconstruction. Furthermore, Saz (2003) developed a 500-year
32 temperature reconstruction for the Ebro Depression (North of Spain), but this chronology is



1 based on a reduced number of cores and a standardized methodology that did not retain the
2 medium and low frequency variance.

3 Here we present the first tree-ring dataset combining samples from three different sources
4 from the eastern IR extending back from the Little Ice Age (1465) to present (2012). The aim
5 of this study is to develop a temperature reconstruction representing the IR, and thereby fill
6 the gap between records located in the northern and southern IP. A new methodology, based
7 on basal area instead of the cambial-age, was applied to preserve high-to-low frequency
8 variance in the resulting chronologies. Furthermore, the relationship between the tree-ring and
9 climate data is reanalysed by adding memory to the climate parameters, since memory effects
10 on tree-ring data are much less acknowledged (Anchukaitis et al., 2012). This analysis is
11 challenging because of the mix of tree species and their unidentified responses to climate. The
12 resulting reconstruction of September maximum temperatures over the past four centuries is
13 compared with latest findings from the Pyrenees and Cazorla, and the relationship with solar
14 and volcanic forcings at inter-annual to multi-decadal timescales.

15

16 **2 Material and methods**

17 **2.1 Site description**

18 We compiled a tree ring network from 11 different sites in the western IR (Table 1) in the
19 province of Soria. Urbión is the most extensive forest of the IP including 120,000 ha between
20 the Burgos and Soria provinces. It has a long forest management tradition. Therefore, all sites
21 are situated at high elevation locations where forests are least exploited and maximum tree
22 age is reached (Fig.1). The altitude of the sampling sites ranges from 1,500 to 1,900 meters
23 above sea level (masl) with a mean of 1,758 masl. These forests belong to the Continental
24 Bioclimatic Belt (Gujarro, 2013) characterized by moderate mean temperatures (9.5°C,
25 Fig.2B) and a large seasonal range including more than 90 frost days and summer heat
26 exceeding 30°C. Mean annual precipitation for the period 1944-2014 is 927 mm (CRU TS.3
27 v.23 dataset by Harris et al., 2014) and reaches its maximum during December (Fig. 2AC).

28 Although scotts pine (*Pinus sylvestris*) is the dominant tree species of the region, other
29 pinaceae are found such as *Pinus pinaster*, *Pinus nigra* or *Pinus uncinata*. Especially
30 remarkable is occurrence of *Pinus uncinata* growing above 1,900 masl and reaching its



1 European southern distribution limits in the IR. The lithology of the study area consists of
2 sandstones, conglomerates and lutites.

3 **2.2 Tree ring chronology development**

4 The new dataset is composed by 316 tree-ring width (TRW) series of *Pinus uncinata* (56) and
5 *Pinus sylvestris* (260) located in the western IR (Tab. 1, Fig. 1). The most recent samples
6 were collected during the field campaign in 2013 including old dominant and co-dominant
7 trees with healthy trunks and no sign of human interference. We extracted two core samples
8 from each tree at breast height (1.3 m) when possible, otherwise, we try to avoid compression
9 wood due to steep slopes, compiling a set of 96 new samples from two sites, i.e. the outermost
10 ring is 2012. Core samples were air-dried and glued onto wooden holders and subsequently
11 sanded to ease growth ring identification (Stokes and Smiley 1968). The samples were then
12 scanned and synchronized using CoRecorder software (Larsson 2012) (Cybis
13 Dendrochronology 2014) to identify the position and exact dating of each ring. The tree-ring
14 width was measured, at 0.01 mm precision, using LINTAB table (Rinn 2005). Prior to
15 detrending, COFECHA (Holmes 1983) was used to assess the cross-dating of all
16 measurement series.

17 An additional set of 95 samples from three sites was provided by the project CLI96-1862
18 (Creus et al. 1992, Saz 2003) i.e., the outermost rings range from 1992 to 1993. Finally, a set
19 of 125 samples from five sites was downloaded from the International Tree Ring Data Bank
20 (ITRDB, <http://www.ncdc.noaa.gov/data-access/paleoclimatology-data/datasets/tree-ring>).
21 These data were developed in the 1980s by K. Richter and collaborators, i.e. the outermost
22 rings range from 1977 to 1985.

23 In order to attempt a climate reconstruction for the western IR from this tree-ring network, we
24 perform an exploratory analysis of the 11 tree-ring chronologies by creating a correlation
25 matrix of the raw chronologies for each site for the common period (1842-1977) and for the
26 full period (1465-2012).

27 **2.2.1 Standardization methods**

28 The key concept in dendroclimatology is referred to as the standardization process (Fritts,
29 1976; Cook et al., 1990) where the aim is to preserve as much of the climate-related
30 information as possible while removing the non-climatic information from the raw TRW



1 measurements. However, with most of the standardization methods a varying proportion of
2 the low-frequency climatic information is also lost in the process (Grudd, 2008). When the
3 aim is to use tree-ring chronologies as a proxy for climatic reconstructions, an adequate
4 standardization is critical and the best method should preserve high to low frequency
5 variations (Büntgen et al., 2004). It is common practice to calculate a mean value function as
6 the best estimate of the trees' signal at a site (Frank et al., 2006).

7 We here applied four standardization methods to the 316 TRW measurement series to develop
8 a single tree-ring index chronology. (i) To emphasize inter-decadal and higher frequency
9 variations, each ring width series was fitted with a cubic spline with a 50% frequency
10 response cut off at 67% of the series length (Cook et al., 1990). A bi-weight robust mean was
11 calculated to assemble the ArstanSTD regional chronology. (ii) A residual chronology
12 (ArstanRES) is produced after removing first-order autoregression to emphasize high-
13 frequency variability. (iii) To preserve common inter-decadal and lower frequency variations,
14 Regional Curve Standardization (RCS) was applied (Mitchell, 1967; Briffa et al., 1992, 1996;
15 Esper et al., 2003). RCS is an age-dependent composite method and involves dividing the size
16 of each tree-ring by the value expected from its cambial age. To assemble the chronology, all
17 the series are aligned by cambial age. A single growth function (regional curve, RC)
18 smoothed using a spline function of 10% of the series length is fit to the mean of all age-
19 aligned series. A biweight robust mean was applied to develop the RCS chronology (RCS).
20 (iv) To preserve high to low frequency variance, we additionally applied a novel
21 standardization method based on the principles of RCS. However, instead of using the
22 cambial age of the trees as the independent variable, we used their sizes, calculated as the
23 square of the basal area of the tree in the year prior to ring formation. Then, a Poisson
24 regression model was used to fit the individual tree-ring widths. Standardized indices were
25 calculated as the ratio between the observed and predicted values, and a biweight robust mean
26 was used to develop the Basal Area Poisson chronology (BasPois).

27 To evaluate uncertainty of the mean chronologies running interseries correlations (R_{bar}) and
28 the express population signal (EPS) were calculated (Wigley et al., 1984). R_{bar} is a measure
29 of the strength of the common growth 'signal' within the chronology (Wigley et al. 1984;
30 Briffa and Jones, 1990), here calculated in a 50-year window sliding along the chronology.
31 EPS is an estimate of the chronology's ability to represent the signal strength of a chronology
32 on a theoretical infinite population (Wigley et al., 1984).



1 **2.3 Climatic data, calibration and climate reconstruction**

2 Monthly temperature (mean, maximum, and minimum) and precipitation values from the
3 gridded CRU TS v.3.22 dataset (0.5° resolution) dataset for the period 1945-2012 were used
4 (Harris et al. 2014). The three grid points closest to the tree-ring network were averaged to
5 develop a regional time series (Fig. 1). In addition, we calculate a cumulative monthly mean
6 for each of the four parameters (max., min., mean temperature, and monthly precipitation).
7 The cumulative mean is calculated by adding the months gradually. First the previous month
8 is added, and then further months are included up to 36 previous months. For the calculations
9 we take into account the current and the previous year.

10 For calibration, we correlated the four chronologies (ArstanSTD, ArstanRES, RCS, and
11 BasPois) with monthly climate data and the cumulative monthly mean derived. To assess the
12 stability of the correlation, we calculated a 30-year moving correlation shifted along 1945-
13 2012 with the cumulative monthly mean from the current and the previous year. In addition,
14 the maximum and minimum differences between the moving correlations were calculated. As
15 a result, the climatic variable chosen for the reconstruction is supported by having the highest
16 moving correlation with the least difference between the maximum and the minimum over the
17 moving correlation period.

18 A split calibration/verification approach was perform over the periods 1945-1978 and 1979-
19 2012 to evaluate the accuracy of the transfer model considering the following metrics;
20 Pearson's correlation (r), coefficient of determination (r^2), reduction of error (RE), mean
21 square error (MSE), and sign test (Cook et al., 1994). R is a measure of the linear correlation
22 between the chronology and climatic variable. R^2 indicates how well the data fit a statistical
23 model. An r^2 of 1 indicates that the regression line perfectly fits the data; an r^2 of 0 indicates
24 that there is not fit at all. RE is a measure of shared variance between actual and estimated
25 series and provides sensitive measure of the reliability of a reconstruction (Cook et al., 1994;
26 Akkemik et al., 2005; Büntgen et al., 2008); it ranges from +1 indicating perfect agreement, to
27 minus infinity. MSE estimates the difference between the modelled and measured while sign
28 test compares the number of agreeing and disagreeing interval trends, from year-to-year,
29 between the observed and reconstructed series (Fritts et al., 1990; Cufar et al., 2008).
30 Additionally, a Superposed Epoch Analysis (SEA; Panofsky and Brier, 1958) was performed
31 using dplR (Bunn, 2008) to assess post-volcanic cooling signals in our reconstruction. The
32 approach has been used in studies of volcanic effect on climate (Fischer et al., 2007; D'Arrigo



1 et al., 2009; Esper et al. 2013a, 2013b). The major volcanic events chosen for the analysis
2 were those identified by Crowley (2000).

3 To transfer the TRW chronology into a temperature reconstruction a linear regression model
4 was used. The magnitude and the spatial extent of the climate signal are evaluated considering
5 the CRU TS v. 3.22 gridded dataset for Europe.

6

7 **3 Results**

8 The correlation matrix (Fig. 3) shows the high inter-correlation between sampling sites and
9 tree species. The highest correlation is found between *Pinus uncinata* (VIN and CAV) located
10 at the highest altitude. On the other hand, the weakest correlation is found between one of the
11 lowest sites (s006) and the highest (VIN). The mean correlation among all sampling sites is r
12 = 0.51 over the common period (1842-1977) is 0.51, and $r = 0.46$ over the full period of
13 overlap, revealing a regionally common, external forcing controlling tree growth and
14 justifying the development of a single chronology integrating the data from this IP tree-ring
15 network.

16 The model (regional curve) of the RCS standardization method and the model of the BasPois
17 method are presented in Fig.4. BasPois model (Fig.4a) indicates a growth of 130 mm when
18 the size of the basal area is near 0 and a growth of 8mm when it reaches the maximum basal
19 area. RCS model (Fig.4b) presents values of 250 mm of growth when the cambial age is 0
20 with a gradual decline of the growth until the cambial of 450. Cambial age from 500 to 550
21 has a slight increase in growth most likely derived by low replication regarding trees with this
22 age.

23 Calibration of the four differently detrended mean chronologies reveals a highly negative
24 correlation with maximum temperatures (Fig. 5). The ArstanRES chronology shows moderate
25 correlations with in previous-year September ($r = -0.25$), and the ArstanSTD chronology
26 correlates at $r = -0.38$ with June and September temperature of the previous year. Considering
27 the RCS chronology, the previous-year September signal increases to $r = -0.49$ with a
28 cumulative monthly mean of 21 months. Finally, the best correlations is revealed for the
29 BasPois chronology reaching $r = -0.78$ with maximum September temperature of the previous
30 year with a cumulative mean of 21 months, which is, in fact a two year cumulative monthly
31 mean. Even though the signals show the same seasonal patterns among the chronologies, the



1 BasPois record always shows the highest correlations. Accordingly, we used the BasPois
2 chronology for the calibration and reconstruction process.

3 The final BasPois network chronology (Fig.6) is based on 316 TRW series of *Pinus uncinata*
4 and *Pinus sylvestris* spanning the 1465-2012 period. Since this chronology is derived from
5 only living trees, mean chronology age increases from 47 years in 1966 to 528 in 1465. The
6 mean sensitivity is 0.21, and first-order autocorrelation 0. The inter-series correlation (R_{bar})
7 reaches 0.26, and the first principal component explains about 35% of the variance. The
8 network chronology's signal to noise ratio is 48.52, and EPS exceeds 0.85 after 1602,
9 constraining the reconstruction period to 410 years until 2012.

10 The selection of the best climate parameter to develop the reconstruction is presented in the
11 Figure 7. Correlations between -0.54 and -0.86 representing only the most significant values
12 are shown. Four parameters reveal the highest correlations over the full calibration period:
13 October of the current year with a cumulative monthly mean of 22 months; September of the
14 previous year with a cumulative monthly mean of 20-months; September of the previous year
15 with a cumulative monthly mean of 21months; and October of the previous year with a
16 cumulative monthly mean of 21 months. The stability of the correlation and therefore the
17 consistency of the signal are tested considering the minimum difference between the
18 maximum and minimum correlation (Fig. 7b) over the full running correlation period. The
19 smallest difference (0.24) is reached for September of the previous year with a cumulative
20 monthly mean of 21months. Therefore, this parameter is chosen for the climate
21 reconstruction. According to the 30-year moving correlations, maximum values are reached
22 from 1973-2003 ($r = -0.80$), whereas the lowest 30-year correlation ($r = -0.60$) is reached from
23 1956-1986. In addition, the relationship between September of the previous year with a
24 cumulative monthly mean of 21months is spatially consistent throughout the Iberian
25 Peninsula, reaching into southern France and northern Africa (Fig.11).

26

27 The transfer model is validated by the high correlation ($r = -0.78$) and significant correlation
28 coefficients ($r^2 = 0.61$) over the full period 1945-2012. Through the split
29 calibration/verification process, considering 1945-1978 and 1979-2012, the temporal
30 robustness was tested revealing highly significant correlations for both periods ($r^2=0.41$ and
31 $r^2=0.55$ respectively) and verifying the final reconstruction (Table 2 and Fig. 8). To develop
32 the final reconstruction spanning 1602-2012, we used a lineal regression model over the full



1 period 1945-2012 with maximum temperature of September of the previous year with a
2 cumulative monthly mean of 21 months (Eq.1), denominated $IR2T_{max}$:

3 $IR2T_{max} = -01533 * BasPoisChron + 2.3542 (r^2_{adj} = 0.61; p < 0.0001)$. (1)

4 **3.1 $IR2T_{max}$ reconstruction**

5 $IR2T_{max}$ describes 410 years of maximum temperature of September with a cumulative
6 monthly mean of 21-months meaning it has memory of the last two years. Temperature
7 ranges from 13.52°C (-2.13°C with respect to the mean) in 1603 to 17.64°C (+1.94°C with
8 respect to the mean) in 2005 (Fig. 9). It is remarkable that the 12 years of the XXI century
9 happen to be within the 25 warmest years. $IR2T_{max}$ covers a part of the Little Ice Age (Grove,
10 1988) from 1602 to the end of the XIX century. The year-to-year temperature variability is
11 3.92°C in the seventeenth century, 2.89°C in the eighteen century, 3.17°C in the nineteenth
12 century and 3.07°C in the twentieth century. The seventeenth and eighteen centuries were the
13 coldest of the reconstruction with 73% and 80% of the years with temperatures below the
14 long-term mean, respectively. On the other hand, the nineteenth and the twentieth centuries
15 were the warmest with 66% and 78% of the years exceeding the mean.

16 The main driver of the large-scale character of the warm and cold episodes may be changes in
17 the solar activity (Fig.9). The beginning of the reconstruction starts with the end of the Spörer
18 Minimum. The Maunder minimum, from 1645 to 1715 (Luterbach et al., 2001) seems to
19 cohere with a cold period from 1645 to 1706. In addition, the Dalton minimum from 1796 to
20 1830, is detected for the period 1810 to 1838. However, a considerably cold period from 1778
21 to 1798 is not in consonance with a decrease in the solar activity. Four warm periods, 1626-
22 1637, 1800-1809, 1845-1859 and 1986-2012, have been identified to cohere with increased
23 solar activity. Overall, the correlation between the reconstruction and the solar activity is 0.34
24 ($p < 0.0001$), and increases to $r = 0.49$ after 11-year low pass filtering the series, though the
25 degrees of freedom are substantially reduced due to the increase autocorrelation.

26 The SEA (Fig.10) indicates some impact of volcanic eruptions on the short-term temperature
27 variability within the reconstruction. It shows significance ($p < 0.05$) decrease in September's
28 temperature with a lag of three years.

29 Figure 11 shows the spatial correlation between the reconstruction and the CRU TS v.3.22 for
30 Europe and northern Africa. High adjusted correlations ($r^2 > 0.4$, $p < 0.0001$) indicate a robust



1 agreement and spatial extend of the reconstruction over the Iberian Peninsula (IP), especially
2 for the central and Mediterranean Spain. The spatial correlation, however, decreases towards
3 the southwest of the IP and the north of Europe.

4

5 **4 Discussion and conclusion**

6 Based on a coherent network of 11 tree-ring sites in the IR including 316 TRW series we
7 developed a 410-year maximum September temperature reconstruction. This record is the first
8 climate reconstruction for the IR filling the gap between the temperature reconstructions
9 developed for the north IP (Büntgen et al., 2008; Dorado-Liñán et al., 2012a, Esper et al.
10 2015a) and for the southern IP (Dorado-Liñán et al, 2014). The IR2T_{max} has been achieved
11 using TRW as well as for the southern IP (Dorado-Liñán et al, 2014). However, for the
12 Pyrenees, MXD (Büntgen et al., 2008, Dorado-Liñán et al., 2012a) or stable isotopes (Esper et
13 al. 2015a) are needed to get skilful records for a temperature reconstruction.

14 The main statistics used to verify the accuracy of the reconstruction present similar values to
15 those developed for the IP. For instance, the best RE coefficient is 0.99 for the split
16 calibration/verification modelled meaning that the reconstruction has almost the perfect skill.
17 A relatively high signal to noise ratio indicates there is meaningful climatic information in the
18 chronology. The mean correlation between sites for the common period ($r = 0.51$, Fig. 3)
19 reveals substantial agreement between the sites and species. Correlation is strongest among
20 high elevation sites including the sites VIN and CAV which are both derived from *Pinus*
21 *uncinata*. The mean chronology, with 35.40% of the first component variance and 48.52 of
22 signal to noise ratio, captures the regional climate signal accurately, which highlights the
23 beauty of regional averages (Briffa et al., 1998).

24 The original, raw chronology extended over the 1465-2012 period, some 150 years longer
25 than the final reconstruction. However, due to low EPS values prior to 1602, which is related
26 to the low number of samples the final reconstruction was developed for the period 1602-
27 2012.

28 A novel detrending approach, considering a Basal Area-Poisson model instead of the
29 traditional regional curve (Esper et al. 2003) has certainly improved the skill of the
30 reconstruction and enabled retaining high-to-low frequency climate variance. The traditional
31 approach of using RCS with the mean TRW curve of the age-aligned data only reached



1 correlations with the maximum temperature of September with a cumulative monthly mean of
2 21 months up to $r = -0.5$, while with the new approach reached $r = -0.78$.

3 It is usually difficult to determine the extent to which the effects of environmental factors on
4 tree growth depend on age (genetic control) and/or on size (physiological control), but recent
5 investigations suggest that it is often the size, and not the age, that is important (Mencuccini et
6 al. 2005; Peñuelas 2005). In fact, climate variability is more size-dependent than age or
7 species (De Luis et al., 2009). Hence, the size-based standardization considered here
8 maximizes the common signal. In addition, when combining TRW series from different sites
9 and species, as done here, the heterogeneity in responses might be large. Therefore, size
10 standardization may be a commendable solution to develop unbiased chronologies. Finally,
11 the new method should be tested in other locations since it may help to maximizes responses
12 especially in heterogeneous areas.

13 Taking into account that TRW growth is conditioned by the storage of starch and sugar in
14 parenchyma ray tissue, the remobilization of carbohydrates from root structures, and the
15 development of needle enduring several growing seasons, influencing the radial increment
16 beyond the instant impact of temperature variability (Pallardy, 2010), we added the
17 cumulative monthly mean to the climate parameters. In fact, we demonstrated that the signal
18 is magnified with a memory of 21 months from the previous September. Thus, developing the
19 two year memory $IR2T_{max}$ allowed us to maintain not only the low frequency signal,
20 highlighting the warm and cold phases, which may be explained by the high correlation with
21 solar activity during 410 years (0.34 , $p < 0.001$), but also the high frequency signal,
22 emphasizing the memory effects of the volcanic eruptions in TRW, already studied by Briffa
23 et al. (1998) and recently by Esper et al. (2015b). According to the SEA (Fig.9), the volcanic
24 eruptions have a significance reduction (95% confidence) of September's temperature ($-$
25 1.98°C) with a three years lag. However, the $IR2T_{max}$ is already considering the two previous
26 year's temperature, which means the temperature decrease occurred the year after the extreme
27 volcanic event in consistency with (Frank et al., 2007a). The stability of the signal was
28 assessed by a 30-y moving correlation from 1945 to 2012, which shows a better correlation
29 for the period 1979-2012 in agreement with the raise of temperatures observed for last
30 decades which may be limiting TRW growth and therefore magnifying the climate signal.
31 However, the relationship between the chronology and the climate parameter chosen never
32 drops from -0.54 within the calibration period 1945-2012. The negative correlation with



1 maximum temperature of previous September is in concordance with the values detected in
2 Cazorla by Dorado-Liñán et al. 2014. Presumably, a continuous rise in temperatures, as
3 suggested by the IPCC (2013), will trigger an incessant decrease in the tree-ring growth.

4 Even though the CRU dataset extends the 1901-2013 period, the general distribution of
5 meteorological observatories in Spain did not begin until the mid-twentieth century
6 (Gonzalez-Hidalgo et al. 2011). In fact, the closest instrumental weather station, located in
7 Vinuesa (Fig.1), began in 1945. However, due to the large amount of gaps in the time series,
8 the CRU dataset was used instead for the split calibration/verification approach for the period
9 1945-2012. The advantages of regional climatic averages were already addressed by Blasing
10 et al. (1981) stating that the average climatic record of the gridded dataset over the study area
11 is representative of the regional climatic conditions, and does not reflect microclimate
12 conditions which may be characteristic of the climatic record at a single station. Tree-ring
13 data might therefore have more variance in common with the regionally averaged climatic
14 record than with the climatic record of the nearest weather station. Generally, studies have
15 shown that the measurements of MXD produce chronologies with an improved climatic signal
16 (Briffa et al., 2002) as it was revealed for summer temperature reconstructions (Hughes et al.,
17 1984; Büntgen et al. 2008; Matskovsky and Helama, 2014). However, based on a TRW
18 chronology, it is remarkable the high correlation coefficient for the full calibration period and
19 the CRU dataset ($r = -0.78$).

20 Throughout the $IR2T_{max}$ reconstruction we identified the main warm and cold phases
21 (Maunder minimum, Dalton minimum) related with long-term temperature variability
22 generally attributed to changes in cycles of activity (Lean et al., 1995; Lassen et al. 1995;
23 Haigh et al. 2015). In addition, similar cold and warm phases are observed comparing with
24 the Pyrenees (Büntgen et al. 2008) and Cazorla (Dorado-Liñán et al. 2014) reconstructions.
25 However, previously to the Dalton minimum, a warm phase is detected in $IR2T_{max}$ and the
26 Cazorla reconstruction although it is not present in the Pyrenees or in the Alps (Büntgen et al.,
27 2011).

28 Through the spatial extent and magnitude of the $IR2T_{max}$ reconstruction over Europe it can be
29 acknowledged that the reconstruction is effective and usable for most of the Spanish Iberian
30 Peninsula. Working especially for the central and Mediterranean IP with very high
31 correlations ($r^2 > 0.4$).

32



1 **Acknowledgements**

2 This study was supported by the Spanish government (CGL2011-28255) and the government
3 of Aragon throughout the Program of research groups (group Clima, Cambio Global y
4 Sistemas Naturales, BOA 147 of 18-12-2002) and FEDER funds. Ernesto Tejedor is
5 supported by the government of Aragon with a Ph.D. grant. Fieldwork was carried out in the
6 province of Soria; we are most grateful to its authorities, for supporting the sampling
7 campaign. We are thankful to Klemen Novak, Edurne Martinez, Luis Alberto Longares, and
8 Roberto Serrano for help during fieldwork.

9



1 5 References

- 2 Akkemik, Ü., Da deviren., N., Aras, A.: A preliminary reconstruction (A.D. 1635–2000) of
3 spring precipitation using oak tree rings in the western Black Sea region of Turkey. *Int J*
4 *Biometeorol* 49(5):297–302, 2005.
- 5 Anchukaitis, K.J., Breitenmoser, P., Briffa, K.R., Buchwal, A., Büntgen, U., Cook, E.R.,
6 D'Arrigo, R.D., Esper, J., Evans, M.N., Frank, D., Grudd, H., Gunnarson, B.E., Hughes,
7 M.K., Kirdyanov, A.V., Körner, C., Krusic, P.J., Luckman, B., Melvin, T.M., Salzer, M.W.,
8 Shashkin, A.V., Timmreck, C., Vaganov, E.A., Wilson, R.J.S.: Tree rings and volcanic
9 cooling. *Nature Geoscience*, 5 (12), pp. 836-837, 2012.
- 10 Barriendos, M.: Climatic variations in the Iberian Peninsula during the late Maunder
11 minimum (AD 1675-1715): An analysis of data from rogation ceremonies. *Holocene*, 7 (1),
12 pp. 105-111, 1997.
- 13 Blasing, T. J., D. N. Duvick, and D. C. West: Dendroclimatic calibration and verification
14 using regionally averaged and single station precipitation data, *Tree-Ring Bulletin*, 41, 37-43,
15 1981.
- 16 Briffa, K.R. and Jones, P.D.: Basic chronology statistics and assessment. In: *Methods of*
17 *Dendrochronology: Applications in the Environmental Sciences* (Eds. E.R. Cook and L.A.
18 Kairiukstis), pp.137-152, 1990.
- 19 Briffa, K.R., Jones, P.D., Bartholin, T.S., Eckstein, D., Schweingruber, F.H., Karlén, W.,
20 Zetterberg, P., Eronen, M.: Fennoscandian summers from ad 500: temperature changes on
21 short and long timescales. *Climate Dynamics*, 7 (3), pp. 111-119, 1992.
- 22 Briffa, K.R., Jones, P.D., Schweingruber, F.H., Osborn, T.J.: Influence of volcanic eruptions
23 on Northern Hemisphere summer temperature over the past 600 years. *Nature*, 393 (6684),
24 pp. 450-455, 1998.
- 25 Briffa, K.R., Osborn, T.J., Schweingruber, F.H., Jones, P.D., Shiyatov, S.G., Vaganov, E.A.:
26 Tree-ring width and density data around the Northern Hemisphere: Part 1, local and regional
27 climate signals. *Holocene*, 12 (6), pp. 737-757, 2002.
- 28 Bunn, A.G.: A dendrochronology program library in R (dplR). *Dendrochronologia* 26:115–
29 124, 2008.

30



- 1 Büntgen, U., Esper, J., Schmidhalter, M., Frank, D.C., Treydte, K., Neuwirth, B., Winiger,
2 M.: Using recent and historical larch wood to build a 1300-year Valais-chronology. In:
3 Gärtner H, Esper J, Schleser G (eds) TRACE 2: 85-92, 2004.
- 4 Büntgen, U., Esper, J., Frank, D.C., Nicolussi, K., Schmidhalter, M.: A 1052-year tree-ring
5 proxy for Alpine summer temperatures. *Climate Dynamics*, 25 (2-3), pp. 141-153, 2005.
- 6 Büntgen, U., Frank, D., Grudd, H., Esper, J.: Long-term summer temperature variations in the
7 Pyrenees. *Climate Dynamics*, 31 (6), pp. 615-631, 2008.
- 8 Camuffo, D., Bertolin, C., Barriendos, M., Dominguez-Castro, F., Cocheo, C., Enzi, S.,
9 Sghedoni, M., della Valle, A., Garnier, E., Alcoforado, M.-J., Xoplaki, E., Luterbacher, J.,
10 Diodato, N., Maugeri, M., Nunes, M.F., Rodriguez, R.: 500-Year temperature reconstruction
11 in the Mediterranean Basin by means of documentary data and instrumental observations.
12 *Climatic Change*, 101 (1), pp. 169-199, 2010.
- 13 Cook, E.R., Briffa, K., Shiyatov, S., Mazepa, V.: Tree-ring standardization and growth trend
14 estimation. In: Cook ER, Kairiukstis LA (eds), *Methods of dendrochronology: applications in
15 the environmental sciences*. Kluwer Academic Publishers, Dordrecht, pp 104–162, 1990.
- 16 Cook, E.R., Briffa, K.R., Jones, P.D.: Spatial regression methods in dendroclimatology: a
17 review and comparison of two techniques. *International Journal of Climatology* 14, 379–402,
18 1994.
- 19 Creus, J. and Puigdefabregas, J.: Climatología histórica y dendrocronología de *Pinus uncinata*
20 R. *Cuadernos de Investigación Geográfica* 2(2): 17-30, 1976.
- 21 Creus, J., Puigdefabregas, J.: Climatología histórica y dendrocronología de *Pinus uncinata* R.
22 *Cuad Investig Geográfica* 2(2):17–30, 1982.
- 23 Crowley, T.J.: Causes of climate change over the past 1000 years. *Science*, 289 (5477), pp.
24 270-277, 2000.
- 25 Čufar, K., de Luis, M., Eckstein, D., Kajfez-Bogataj, L.: Reconstructing dry and wet summers
26 in SE Slovenia from oak tree-ring series. *Int J Biometeorol* 52:607–615, 2008.
- 27 D'Arrigo, R., Wilson, R., Tudhope, A.: The impact of volcanic forcing on tropical
28 temperatures during the past four centuries. *Nature Geoscience*, 2 (1), pp. 51-56, 2009.



- 1 de Luis, M., Novak, K., Čufar, K., Raventós, J.: Size mediated climate-growth relationships in
2 *Pinus halepensis* and *Pinus pinea*. *Trees - Structure and Function*, 23 (5), pp. 1065-1073,
3 2009.
- 4 Domínguez-Castro, F., García-Herrera, R., Ribera, P., Barriendos, M.: A shift in the spatial
5 pattern of Iberian droughts during the 17th century. *Climate of the Past*, 6 (5), pp. 553-563,
6 2010.
- 7 Dorado Liñán, I., Büntgen, U., González-Rouco, F., Zorita, E., Montávez, J.P., Gómez-
8 Navarro, J.J., Brunet, M., Heinrich, I., Helle, G., Gutiérrez, E.: Estimating 750 years of
9 temperature variations and uncertainties in the Pyrenees by tree-ring reconstructions and
10 climate simulations. *Climate of the Past*, 8 (3), pp. 919-933, 2012.
- 11 Dorado Liñán, I., Zorita, E., González-Rouco, J.F., Heinrich, I., Campello, F., Muntán, E.,
12 Andreu-Hayles, L., Gutiérrez, E.: Eight-hundred years of summer temperature variations in
13 the southeast of the Iberian Peninsula reconstructed from tree rings. *Climate Dynamics*, 44 (1-
14 2), pp. 75-93, 2014.
- 15 El Kenawy, A., López-Moreno, J.I., Vicente-Serrano, S.M.: Trend and variability of surface
16 air temperature in northeastern Spain (1920-2006): Linkage to atmospheric circulation.
17 *Atmospheric Research*, 106, pp. 159-180, 2012.
- 18 Esper, J., Cook, E.R., Krusic, P.J., Peters, K., Schweingruber, F.H.: Tests of the RCS method
19 for preserving low-frequency variability in long tree-ring chronologies. *Tree-Ring Research*
20 59, 81-98, 2003.
- 21 Esper, J., Büntgen, U., Luterbacher, J., Krusic, P.: Testing the hypothesis of post-volcanic
22 missing rings in temperature sensitive dendrochronological data. *Dendrochronologia* 13, 216-
23 222, 2013.
- 24 Esper, J., Schneider, L., Krusic, P.J., Luterbacher, J., Büntgen, U., Timonen, M., Sirocko, F.,
25 Zorita, E.: European summer temperature response to annually dated volcanic eruptions over
26 the past nine centuries. *Bulletin of Volcanology* 75, 2013.
- 27 Esper, J., Großjean, J., Camarero, J.J., García-Cervigón, A.I., Olano, J.M., González-Rouco,
28 J.F., Domínguez-Castro, F., Büntgen, U.: Atlantic and Mediterranean synoptic drivers of
29 central Spanish juniper growth. *Theoretical and Applied Climatology*, 2014.



- 1 Esper, J., Konter, O., Krusic, P., Saurer, M., Holzkämper, S., Büntgen, U.: Long-term summer
2 temperature variations in the Pyrenees from detrended stable carbon isotopes.
3 *Geochronometria* 42, 53-59, 2015.
- 4 Esper, J., Schneider, L., Smerdon, J.E., Schöne, B.R., Büntgen, U.: Signals and memory in
5 tree-ring width and density data. *Dendrochronologia*, 35, pp. 62-72, 2015b.
- 6 Fischer, E.M., Luterbacher, J., Zorita, E., Tett, S.F.B., Casty, C., Wanner, H.: European
7 climate response to tropical volcanic eruptions over the last half millennium, *Geophys. Res.*
8 *Let.*, 34, L05707, 2007.
- 9 Frank, D., Esper, J., Cook, E.R.: On variance adjustments in tree-ring chronology
10 development. In: Heinrich I et al. (Eds.) *Tree rings in archaeology, climatology and ecology*,
11 *TRACE*, Vol. 4, 56-66, 2006.
- 12 Frank, D., Büntgen, U., Böhm, R., Maugeri, M., Esper, J.: Warmer early instrumental
13 measurements versus colder reconstructed temperatures: shooting at a moving target.
14 *Quaternary Science Reviews* 26, 3298-3310, 2007a.
- 15 Fritts, H.C., Guiot, J., Gordon, G.A., Schweingruber, F.H.: Methods of calibration,
16 verification, and reconstruction. In *Methods of Dendrochronology*, 1990.
- 17 Fritts, H.C.: *Tree rings and climate*. Academic Press, London, 1976.
- 18 Giorgi, F., Lionello, P.: Climate change projections for the Mediterranean region, *Global and*
19 *Planetary Change*, Volume 63, Issues 2–3, September, Pages 90-104, 2008.
- 20 González-Hidalgo, J.C., Brunetti, M., de Luis, M.: A new tool for monthly precipitation
21 analysis in Spain: MOPREDAS database (monthly precipitation trends December 1945
22 November 2005). *International Journal of Climatology*, 31 (5), pp. 715-731, 2011.
- 23 Gonzalez-Hidalgo, J.C., Peña-Angulo, D., Brunetti, M., Cortesi, N. MOTEDAS: A new
24 monthly temperature database for mainland Spain and the trend in temperature (1951-2010).
25 *International Journal of Climatology*, 2015.
- 26 Grudd, H.: Torneträsk tree-ring width and density ad 500-2004: A test of climatic sensitivity
27 and a new 1500-year reconstruction of north Fennoscandian summers. *Climate Dynamics*, 31
28 (7-8), pp. 843-857, 2008.
- 29 Guijarro, J.A.: Tendencias de la temperatura en España. En García Legaz, C. y Valero, C.
30 (Coords). *Fenómenos meteorológicos adversos en España*. AEMET y CCS. Madrid, 2013.



- 1 Haigh, J.D., Cargill, P.: The Sun's Influence on Climate, pp. 1-207, 2015.
- 2 Harris, I., Jones, P.D., Osborn, T.J., Lister, D.H.: Updated high-resolution grids of monthly
3 climatic observations - the CRU TS3.10 Dataset. *International Journal of Climatology*, 34 (3),
4 pp. 623-642, 2014.
- 5 Hertig, E. and J. Jacobeit: Assessments of Mediterranean precipitation changes for the 21st
6 century using statistical downscaling techniques. *International Journal of Climatology* 28(8):
7 1025-1045, 2008.
- 8 Holmes, R.L.: Computer-assisted quality control in tree-ring dating and measurement. *Tree-
9 Ring Bull* 43:69–78, 1983.
- 10 Hughes, M.K., Schweingruber, F.H., Cartwright, D., Kelly, P.M.: July-August temperature at
11 Edinburgh between 1721 and 1975 from tree-ring density and width data. *Nature*, 308 (5957),
12 pp. 341-344, 1984
- 13 IPCC, 2013: *Climate Change 2013: The Physical Science Basis*. Contribution of Working
14 Group I to the Fifth Assessment Report of the Intergovernmental Panel on Climate Change
15 [Stocker, T.F., D. Qin, G.-K. Plattner, M. Tignor, S.K. Allen, J. Boschung, A. Nauels, Y. Xia,
16 V. Bex and P.M. Midgley (eds.)]. Cambridge University Press, Cambridge, United Kingdom
17 and New York, NY, USA, 1535 pp, doi:10.1017/CBO9781107415324.
- 18 Larsson, L.A.: CoRecorder&CDendro program. Cybis Elektronik & Data AB. Version 7.6,
19 2012.
- 20 Lassen, K., Friis-Christensen, E.: Variability of the solar cycle length during the past five
21 centuries and the apparent association with terrestrial climate. *Journal of Atmospheric and
22 Terrestrial Physics*, 57 (8), pp. 835-845, 1995.
- 23 Lean, J., Beer, J., Bradley, R.: Reconstruction of solar irradiance since 1610: implications for
24 climate change. *Geophysical Research Letters*, 22 (23), pp. 3195-3198, 1995.
- 25 Lionello, P., Malanotte-Rizzoli, P., Boscolo, R., Alpert, P., Artale, V., Li, L., Luterbacher, J.,
26 May, W., Trigo, R., Tsimplis, M., Ulbrich, U., Xoplaki, E.: The Mediterranean climate: An
27 overview of the main characteristics and issues. *Developments in Earth and Environmental
28 Sciences*, 4 (C), pp. 1-26, 2006a.
- 29 López-Moreno, J.I., El-Kenawy, A., Revuelto, J., Azorín-Molina, C., Morán-Tejeda, E.,
30 Lorenzo-Lacruz, J., Zabalza, J., Vicente-Serrano, S.M.: Observed trends and future



- 1 projections for winter warm events in the Ebro basin, northeast Iberian Peninsula.
2 International Journal of Climatology, 34 (1), pp. 49-60, 2014.
- 3 Luterbacher, J., Rickli, R., Xoplaki, E., Tinguely, C., Beck, C., Pfister, C., Wanner, H.: The
4 Late Maunder Minimum (1675-1715) - A key period for studying decadal scale climatic
5 change in Europe. Climatic Change, 49 (4), pp. 441-462, 2001.
- 6 Luterbacher, J., Xoplaki, E., Casty, C., Wanner, H., Pauling, A., Küttel, M., Rutishauser, T.,
7 Brönnimann, S., Fischer, E., Fleitmann, D., Gonzalez-Rouco, F.J., García-Herrera, R.,
8 Barriendos, M., Rodrigo, F., Gonzalez-Hidalgo, J.C., Saz, M.A., Gimeno, L., Ribera, P.,
9 Brunet, M., Paeth, H., Rimbu, N., Felis, T., Jacobeit, J., Dünkeloh, A., Zorita, E., Guiot, J.,
10 Türkes, M., Alcoforado, M.J., Trigo, R., Wheeler, D., Tett, S., Mann, M.E., Touchan, R.,
11 Shindell, D.T., Silenzi, S., Montagna, P., Camuffo, D., Mariotti, A., Nanni, T., Brunetti, M.,
12 Maugeri, M., Zerefos, C., Zolt, S.D., Lionello, P., Nunes, M.F., Rath, V., Beltrami, H.,
13 Garnier, E., Ladurie, E.L.R.: Chapter 1 Mediterranean climate variability over the last
14 centuries: A review, 2006.
- 15 Matskovsky, V.V., Helama, S.: Testing long-term summer temperature reconstruction based
16 on maximum density chronologies obtained by reanalysis of tree-ring data sets from
17 northernmost Sweden and Finland. Clim.Past 10, 1473–1487, 2014.
- 18 Mencuccini, M., Martínez-Vilalta, J., Vanderklein, D., Hamid, H.A., Korakaki, E., Lee, S.,
19 Michiels, B.: Size-mediated ageing reduces vigour in trees. Ecology Letters, 8 (11), pp. 1183-
20 1190, 2005.
- 21 Mitchell, V.L.: An investigation of certain aspects of tree growth rates in relation to climate in
22 the central Canadian boreal forest. Technical report 33pp. Department of Meteorology,
23 University of Wisconsin, 1967.
- 24 Pallardy, S.G.: Physiology of Woody Plants. Academic Press, 2010.
- 25 Panofsky, H.A., Brier, G.W.: Some applications of statistics to meteorology. University Park,
26 Pennsylvania, p. 224, 1958.
- 27 Pena-Angulo, D., Cortesi, N., Brunetti, M., González-Hidalgo, J.C.: Spatial variability of
28 maximum and minimum monthly temperature in Spain during 1981–2010 evaluated by
29 correlation decay distance (CDD). Theoretical and Applied Climatology, 122 (1-2), pp. 35-45,
30 2015.



- 1 Peñuelas, J.: Plant physiology—a big issue for trees. *Nature*, 437:965–966, 2005.
- 2 Rinn, F.: TSAPWinTM – Time series analysis and presentation for dendrochronology and
3 related applications, Version 4.69, 2005.
- 4 Ruiz, P.: Análisis dendroclimático de *Pinus uncinata Ramond* en la Sierra Cebollera (Sistema
5 Ibérico). *Cuadernos de Investigación Geográfica* 15(1-2): 75-80, 1989.
- 6 Ruiz-Flaño, P.: Dendroclimatic series of *Pinus uncinata* R. in the Central Pyrenees and in the
7 Iberian System. A comparative study. *Pirineos* 132:49–64, 1988.
- 8 Sánchez, E., Gallardo, C., Gaertner, M.A., Arribas, A., Castro, M.: Future climate extreme
9 events in the Mediterranean simulated by a regional climate model: A first approach. *Global
10 and Planetary Change*, 44 (1-4), pp. 163-180, 2004.
- 11 Saz, M.A.: Análisis de la evolución del clima en la mitad septentrional de España desde el
12 siglo XV a partir de series dendroclimáticas. Servicio de Publicaciones de la Universidad de
13 Zaragoza, Zaragoza, 1105 pp, 2003.
- 14 Smith, J. G. and Weston, H. K.: Nothing particular in this year's history, *J. Oddball Res.*, 2,
15 14-15, 1954.
- 16 Smith, J. G. and Weston, H. K.: Nothing particular in this year's history, *J. Oddball Res.*, 2,
17 14-15, 1954.
- 18 Stokes, M.A., Smiley, T.L.: An introduction to tree-ring dating, 2nd edn. The University of
19 Arizona Press, Tucson, 1968.
- 20 Tejedor, E., de Luis, M., Cuadrat, J.M., Esper, J., Saz, M.Á.: Tree-ring-based drought
21 reconstruction in the Iberian Range (east of Spain) since 1694. *International Journal of
22 Biometeorology*, 12 p, 2015.
- 23 Vicente-Serrano, S.M. and Cuadrat, J.M.: North Atlantic oscillation control of droughts in
24 north-east Spain: Evaluation since 1600 A.D. *Climatic Change*, 85 (3-4), pp. 357-379, 2007.
- 25 Wigley, T.M.L., Briffa, K., Jones, P.D.: On the average value of correlated time series, with
26 applications in dendroclimatology and hydrometeorology. *J Clim Appl Meteorol* 23:201–213,
27 1984.
- 28
- 29



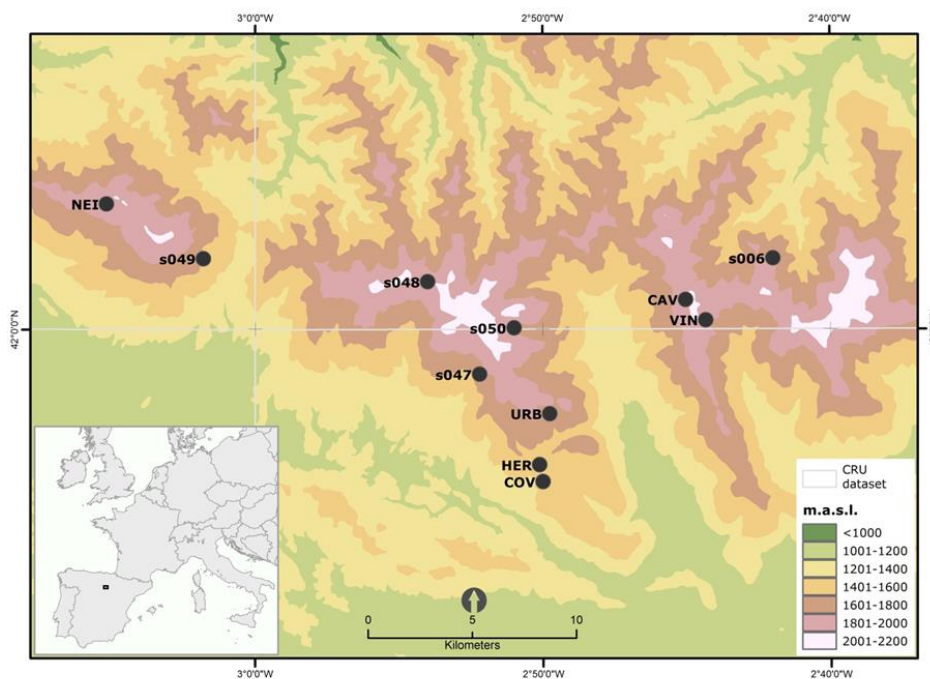
1 Table 1. Tree ring sites characteristics

Code	Site	Source	Lat	Long	Elevation	Species	Tree no	Sample no	Tree-rings	Period
s047	Urbión Covaleda	ITRDB	41.98	-2.87	1750	PISY	15	31	6549	1567- 1983
s048	Urbión Duruelo	ITRDB	42.02	-2.90	1840	PISY	8	17	3590	1671- 1983
s049	Urbión Quintenar	ITRDB	42.03	-3.03	1840	PISY	12	27	4713	1593- 1985
s050	Urbión Vinuesa	ITRDB	42.00	-2.85	1750	PISY	4	8	1942	1681- 1983
s006	Urbión	ITRDB	42.03	-2.7	1634	PISY	11	22	2397	1842- 1977
CAV	Castillo de Vinuesa	UNIZAR	42.01	-2.75	1900	PIUN	18	36	9236	1593- 2012
COV	Covaleda	IPE- CSIC- UNIZAR	41.93	-2.83	1500	PISY	16	48	14696	1568- 1993
HER	Barranco de las heridas	IPE- CSIC- UNIZAR	41.94	-2.84	1500	PISY	25	32	9347	1562- 1993
NEI	Neila	IPE- CSIC- UNIZAR	42.05	-3.08	1850	PISY	9	15	4822	1587- 1992



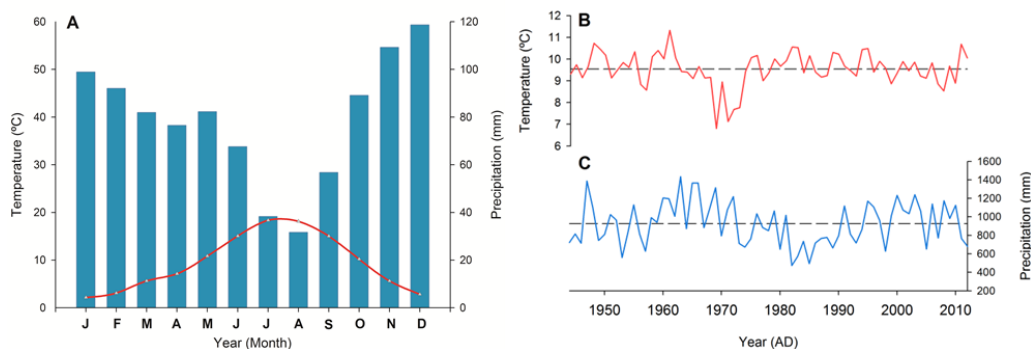
URB	Picos de Urbi3n	de UNIZAR	41.96	-2.82	1750	PISY	28	60	11328	1733-2012
VIN	Castillo de Vinuesa	IPE-CSIC-UNIZAR	42.03	-2.73	1900	PIUN	13	20	7653	1465-1992
Total							159	316	76273	

1 UNIZAR University of Zaragoza, IPE-CSIC Spanish National Research Council, ITRDB International Tree-Ring
 2 Databank

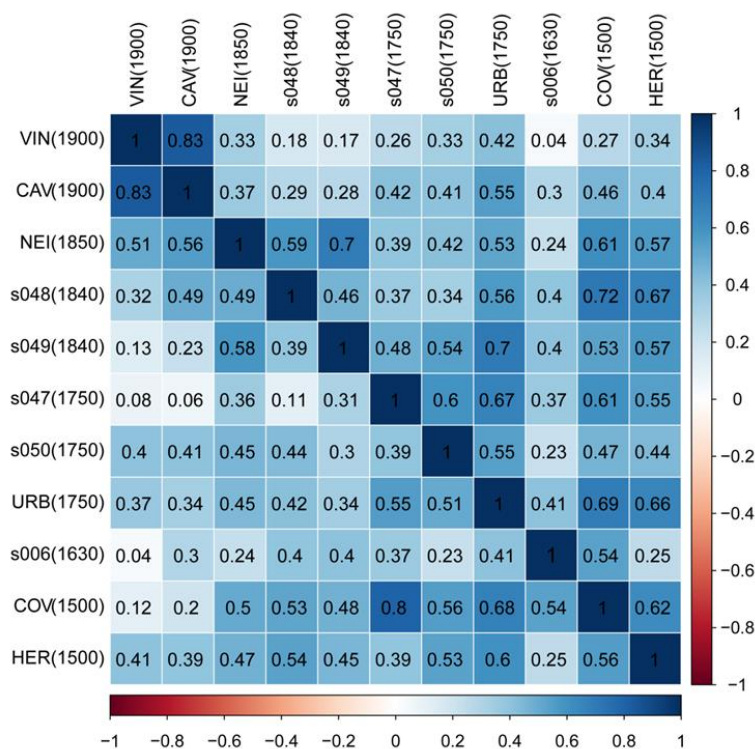


3
 4 Figure 1. Map showing the tree ring study sites and the climate data (CRU TS v.3.22) grid
 5 points in the Western Iberian Range (Soria).

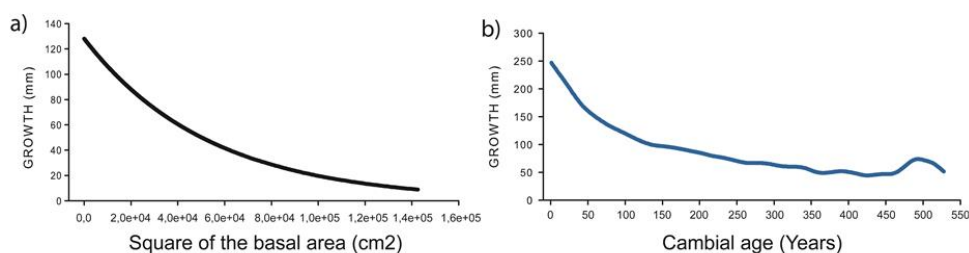
6
 7
 8
 9



1
 2 Figure 2. Climate diagram (A), mean temperature (B), mean precipitation (C) calculated using
 3 data from CRU TS v.3.22 over the period 1944-2012 (Harris et al 2014).

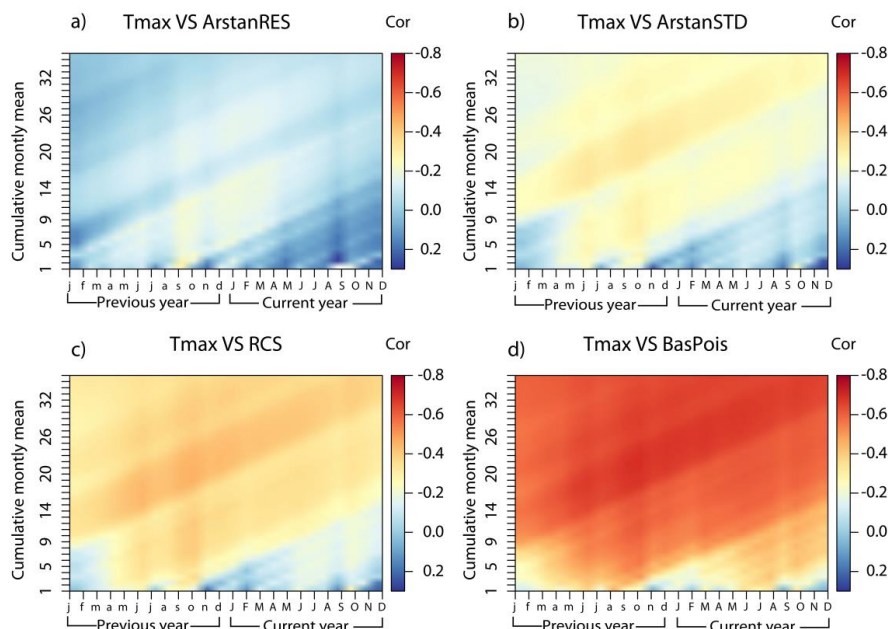


4
 5 Figure 3. Correlation of the raw chronologies sorted by elevation. Top right shows the
 6 correlations calculated over the common period 1842-1977. Bottom left shows the correlation
 7 over the full period of overlap between pairs of chronologies



1

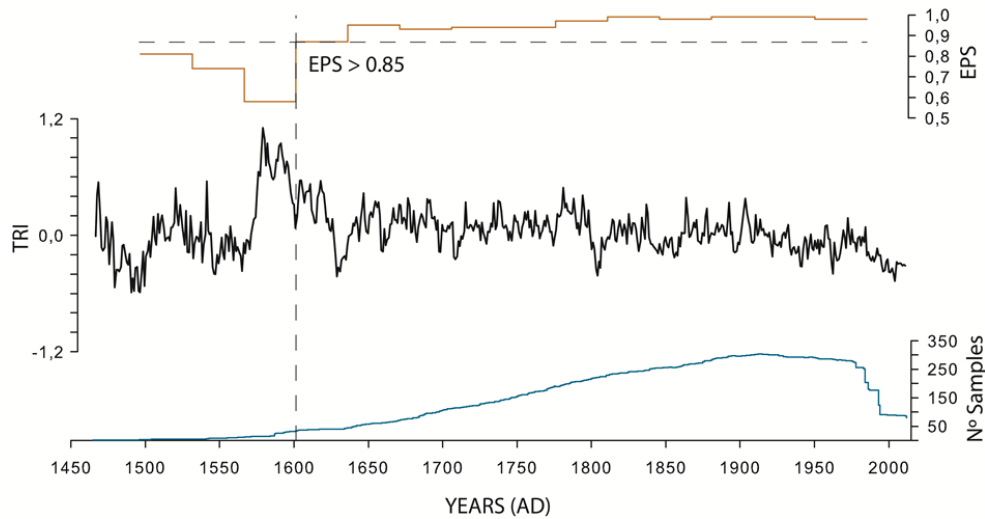
2 Figure 4. a) Represents the model of the BasPois method, b) represents the regional curve of
 3 the RCS method.



4

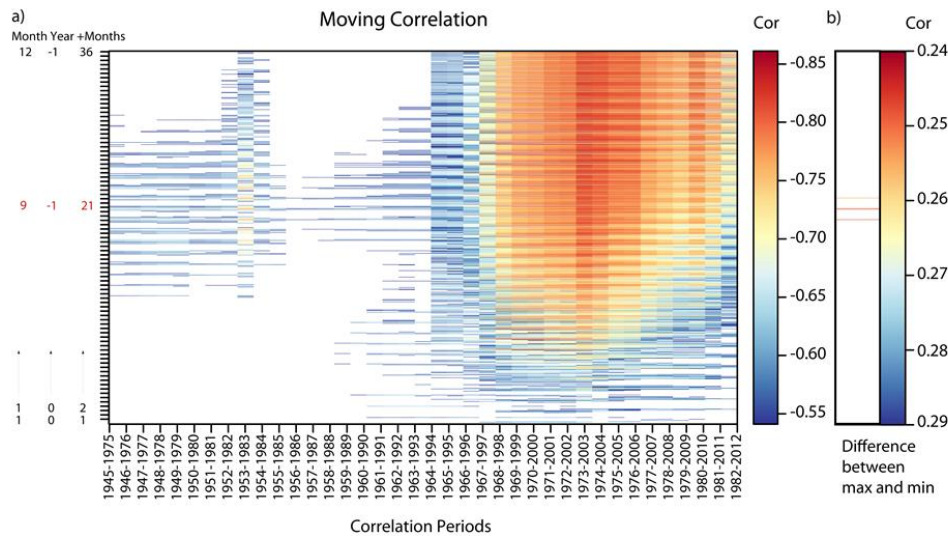
5 Figure 5. Correlation between the maximum temperature (from January of the previous year
 6 to December of the current year with a cumulative monthly mean from 1 to 36 months) and
 7 the residual Arstan chronology (a), the standard Arstan chronology (b), the RCS standard
 8 chronology (c) and the Basal Area-Poisson standard chronology (d).

9



1

2 Figure 6. BasPois chronology (in black), number of samples (blue) and EPS statistic
 3 (computed over 30-y window lagged by 15 years) back to 1465. Vertical dashed line
 4 highlights the EPS=0.85 threshold in 1602.



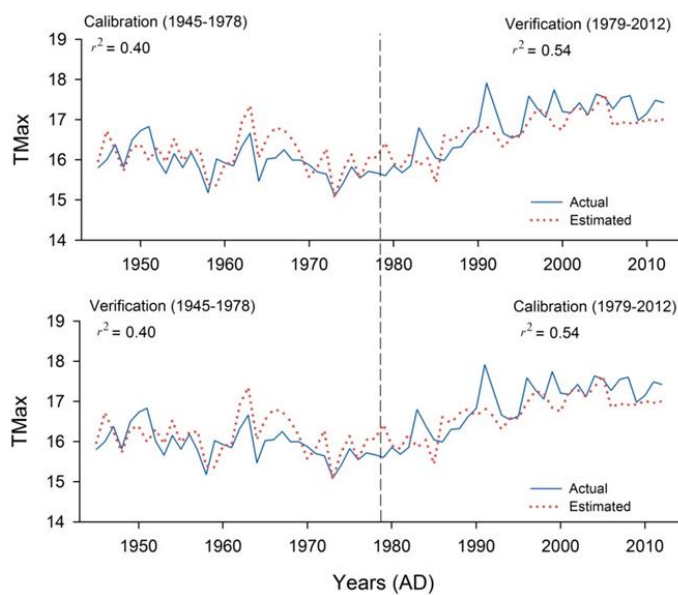
5

6 Figure 7.a) 30-year moving correlation from 1945 to 2012 between the maximum
 7 temperature, from January of the current year (1,0,1) to December of the previous year (12, -
 8 1, 36) with a cumulative monthly mean from 1 to 36 months and the BasPois chronology. Red
 9 numbers indicates the chosen climatological parameter; 9, September, -1, previous year, 21,

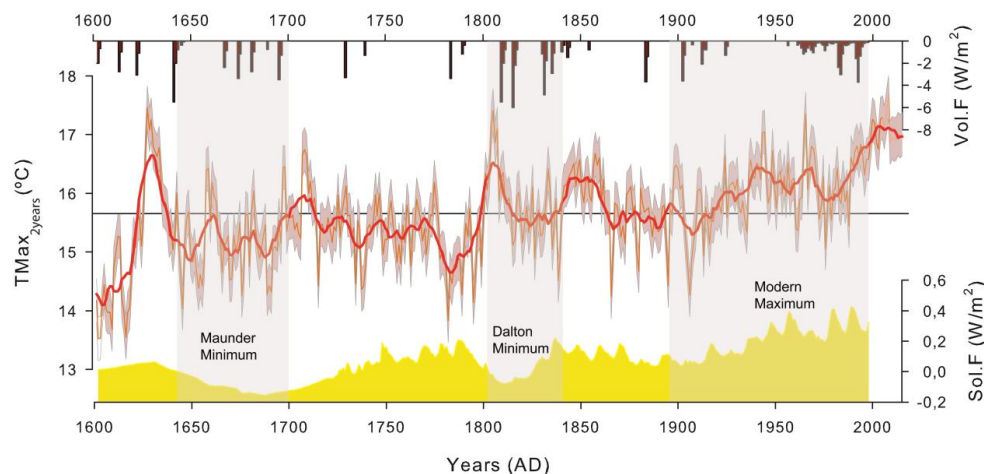


1 months used for the cumulative monthly mean. b) The four best parameters are represented.
2 Reddish line indicates the least difference between the maximum and minimum correlation in
3 the correlation periods.

4
5
6
7
8
9
10
11
12
13
14
15
16
17
18
19



20 Figure 8. Calibration and verification results of the CRU data based $T_{max_{Sep-1}}$ reconstruction
21
22
23



1 Figure 9. IR2T_{max} reconstruction since AD 1602 for the Iberian Range. Bold red curve is a 11-
 2 year running mean, purple shading indicates the mean square error based on the calibration
 3 period correlation. Yellow shading at the bottom show solar forcing and bars on top indicate
 4 volcanic forcings (Crowley 2000).

5

	Calibration 1945-1978	Verification 1978-2012	Calibration 1979-2012	Verification 1945-1978	Period 1945-2012
Years	34	34	34	34	68
Correlation	-0.64	0.73	-0.74	0.64	-0.78
R ² _{adj}	0.40	0.54	0.54	0.40	0.61
MSE	0.09	0.66	0.18	0.29	0.37
Reduction of error	0.99	0.99	0.99	0.99	0.99
Sing test	28+/6-	24+/10-	28+/6-	24+/10-	52+/16-

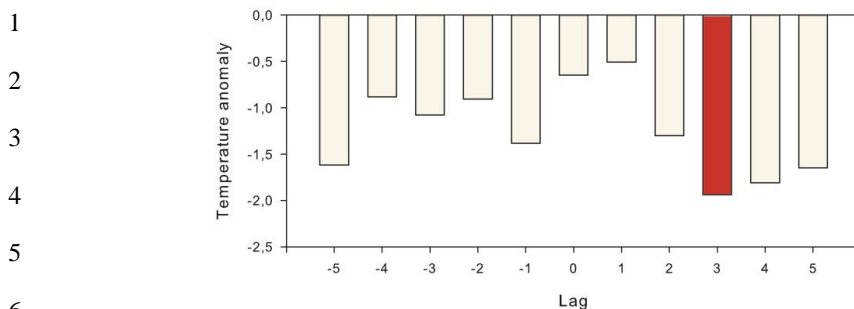
6 Table 2. Calibration/verification statistics of the T_{max}_{Sep-1} reconstruction

7

8

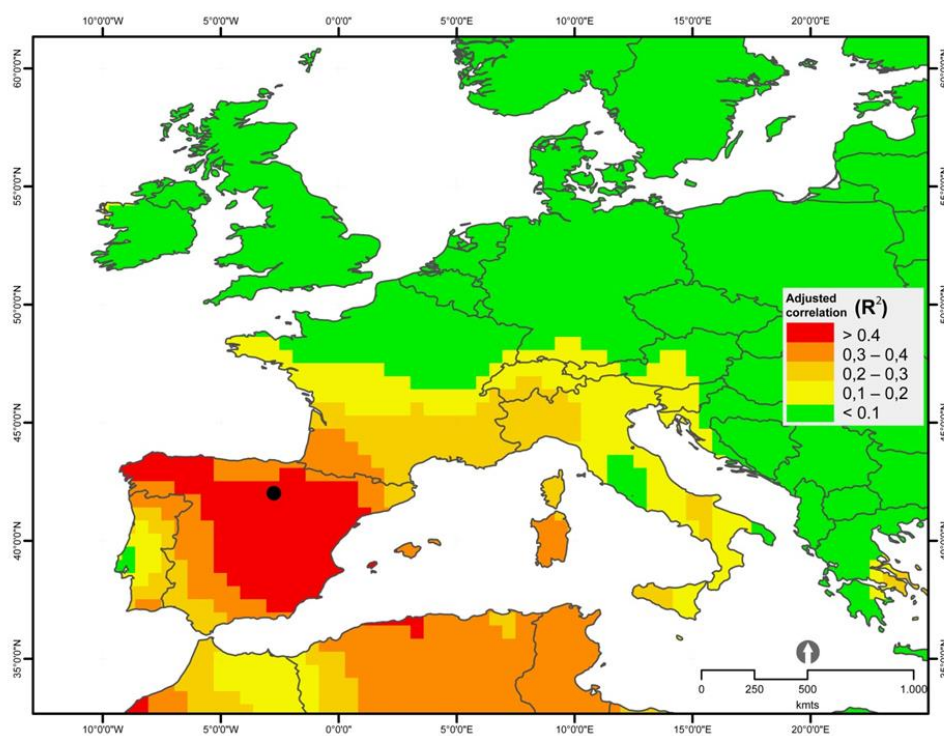
9

10



7 Figure 10. Superposed epoch analysis with a back and forward lag of 5 years. Significance
8 ($p < 0.05$) at 3 years after the extreme volcanic event.

9



10

11 Figure 11. Map showing the spatial correlation patterns of the BasPois chronology with the
12 gridded September of the previous year with a cumulative monthly mean of 21 months data.
13 Correlation values are significant at $p < 0.0001$.

14